

Topological phase of many-body non-Hermitian systems

Kui Cao and Su-Peng Kou*

Center for Advanced Quantum Studies, Department of Physics,
Beijing Normal University, Beijing 100875, China

We show that free many-body fermionic non-Hermitian systems require two distinct sets of topological invariants to describe the topology of energy bands and states respectively, with the latter yet to be explored. We identify 10 symmetry classes—defined by particle-hole, linearized time-reversal, and linearized chiral symmetries, leading to a 10-fold classification for quantum states of many-body non-Hermitian topological phase. Unique topological invariants are defined in each class, dictating the topology of states. These findings pave the way for deeper understanding of the topological phases of many-body non-Hermitian systems.

Introduction.—Quantum Hall effect inspired developments have ushered in the topological phases paradigm for phase classification and description [1–19]. In these phases, an underlying foundation is laid by internal symmetries, independent of specific spatial constructs. In Hermitian systems, primary internal symmetries fuse in the form of Altland-Zirnbauer (AZ) symmetry—time-reversal symmetry (TRS), particle-hole symmetry (PHS), and chiral symmetry (CS), leading to a suite of 10 symmetry classes [20]. Quantum states belonging to different topological phases cannot be transformed into each other by local unitary transformations that do not break certain AZ symmetries [21–25]. Therefore, different topological phases are certainly linked by phase transitions [21, 22]. The topological phase is classified and described by a topological invariant defined in its specific symmetry class, and all unique properties of topological phases, such as gapless modes under open boundaries and quantum entanglement entropy, are characterized by the system’s topological invariant [26–28]. The confines of Hermitian systems have been extended in recent years, as the inclusion of non-Hermitian effects has led to an expanded lattice of 38 symmetry classes, incorporating TRS, PHS, CS, and three related Hermitian conjugates [29–31]. In these classes, topological invariants assign distinct systems, which changes tied to gap closures.

The effectiveness of this expanded classification framework is unquestionable in the context of band structures. However, the question remains whether it can also classify and describe the quantum states—defined as the steady-state under time evolution of many-body non-Hermitian systems. In non-Hermitian physics, the transition between quantum states of different phases does not necessarily occur at the band gap closure [32, 33]. This implies that the phase diagram of quantum states may not be bounded by gap closure points—while the topological phase diagram determined by the 38-fold classification is definitely bounded by gap closure points. Addressing these concerns, our study raises two pivotal questions: Can the existing framework classify the quantum states of many-body non-Hermitian systems? If not, what al-

ternative approach can categorize the state of topological phases? In this letter, we use a one-dimensional topological insulator at finite temperatures as an example, leading to the discovery of phase transitions independent of gap closures, suggesting a unique property of such system: the independent presence of states topology and energy band topology. This discrepancy also indicates that the state of topology need necessitating distinct classification schemes.

In light of these findings, we propose a new classification approach that leads to a 10-fold classification for many-body non-Hermitian system’s states base on particle-hole symmetry and linearized time-reversal symmetry and linearized chiral symmetry of Hamiltonians. Each class herein yields its distinct topological invariant, and transitions between systems with different topological invariants necessitate phase transitions, which are not invariably tied to gap closures. Notably, systems with skin effects do not subscribe to the classifications within these ten classes, they lacking a well-defined topological invariant. Through this unveiling, we hope to advance the understanding of topological many-body non-Hermitian systems.

Phase transition in non-Hermitian topological phase.—We begin with a 1D non-Hermitian model of which Hamiltonian is

$$\begin{aligned} \hat{H}_{\text{NH}} = & \sum_i^L U \psi_i^\dagger \sigma_z \psi_i + \frac{1}{2} \sum_i^{L-1} t (\psi_i^\dagger \psi_{i+1} + \psi_{i+1}^\dagger \psi_i) \\ & + \frac{1}{2} \sum_i^{L-1} (J + \gamma) (\psi_i^\dagger \sigma_+ \psi_{i+1} + \psi_{i+1}^\dagger \sigma_+ \psi_i) \\ & + \frac{1}{2} \sum_i^{L-1} (J - \gamma) (\psi_i^\dagger \sigma_- \psi_{i+1} + \psi_{i+1}^\dagger \sigma_- \psi_i), \end{aligned} \quad (1)$$

where $\psi_i = (a_i, b_i)^T$, a_i and b_i are the annihilation operators of fermions on sublattices a and b , respectively. $\sigma_{x,y,z}$ are pauli matrices and $\sigma_{+,-} = \frac{1}{2}(\sigma_x \pm i\sigma_y)$ are raising/lowering operators. J, U, t , and γ are all real numbers. We set $J, t > 0$. The schematic diagram of the model is shown in Fig. 1. We consider cases where γ is less than J . In this study, we only consider half-

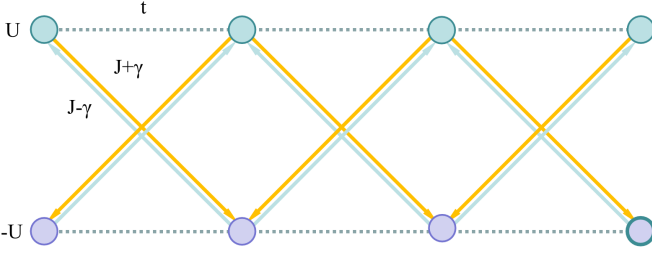


FIG. 1. Schematic diagram of the non-Hermitian topological insulator.

filled systems, i.e., systems with a particle number of L . The above system implementation can be experimentally achieved using ultracold atoms in optical lattices combined with the methodically engineered dissipation proposed in Ref. [34], supplemented by an auxiliary thermal cavity to obtaining a controllable temperature.

In this model, the absence of the skin effect signifies that its characteristics can be described using the Bloch Hamiltonian, represented as

$$H(k) = (U - t \cos k) \sigma_z + J \sin k \sigma_y + i\gamma \sin k \sigma_x. \quad (2)$$

The gap of the system is

$$\Delta = 2\sqrt{J^2 - \gamma^2 + (t^2 + U^2 - J^2 + \gamma^2) \cos^2 k - 2Ut \cos k},$$

which closes at $U_{g\pm} = \pm t$.

We examine the quantum states of this model. As practical many-body systems often have temperature due to coupling with the environment, we couple the system with a heat bath at temperature $T \equiv \frac{1}{\beta}$ to study its physics under finite temperature. We set the coupling term as $\hat{H}_{BS} = \sum_i (\lambda_i^1 a_i^\dagger a_i \otimes \hat{B}_i^1 + \lambda_i^2 b_i^\dagger b_i \otimes \hat{B}_i^2)$. Here, λ_i^1, λ_i^2 is a small real coupling constant and \hat{B}_i^1, \hat{B}_i^2 is an operator in thermal bath B. We define that the non-Hermitian system has the same temperature as the thermal bath B at the steady state. Conversely, when the system evolves to its steady state, its temperature approaches T . We obtain the density matrix at temperature T as [35, 36]

$$\rho = e^{-\beta \hat{H}_{NH}} e^{\ln \frac{J \pm \gamma}{J \mp \gamma} \sum_i \psi_i^\dagger \sigma_z \psi_i}. \quad (3)$$

Here, all operators are confined within the Fock subspace characterized by a particle number of L . Subsequent calculations of the model's revealed a phase transition, as indicated by the the first derivative of the logarithm of the partition function $\frac{d}{dT} \ln \text{tr} \rho$ undergoes a sudden change. Interestingly, this phase transition did not align with the closure of the system gap. The phase transition occurs at

$$U_{c\pm} = \frac{T}{2} \ln \frac{J + \gamma}{J - \gamma} \pm t. \quad (4)$$

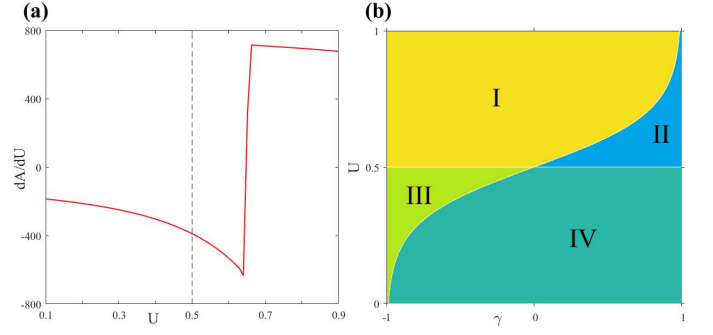


FIG. 2. (a) The derivative of $A \equiv \ln \text{tr} \rho$, evaluated at $T = 0.5$, $t = 1$ and $\gamma = 0.3$. (b) Phase diagram at $T = 0.1$.

which is different from the system's band gap closing points $U_{g\pm}$, see Fig. 2. This implying a phase transition has occurred in the system without closing the gap.

Phase diagram for non-Hermitian topological system.—The band closure points and phase transition critical points divide the phase diagram into four regions, as shown in Fig. 2(b). To understand the significance of the regions in the phase diagram, we analyze the implications of the two lines.

Firstly, we analyze the physical significance of the band closing point. We note that zero modes appear among the two band closing points. See Fig. 2(b) for one scenario. The appearance of zero modes is described by the topological invariant within the 38-fold classification. A winding number $W = 1$ characterizes a topological phase when $U_{g-} < U < U_{g+}$, while $W = 0$ denotes a trivial phase when $U > U_{g+}$ or $U < U_{g-}$. Secondly, we analyze the physical significance of the phase transition critical points. We take note that the density matrix of the system remains gaussian, and thus can be expressed in the form of $\rho = e^{-\beta \sum_k \psi_k^\dagger H_{\text{eff}}(k) \psi_k}$, where

$$H_{\text{eff}}(k) = \frac{W(k)}{\sqrt{A_y(k)^2 + A_z(k)^2}} [A_y(k) \sigma_y + A_z(k) \sigma_z].$$

where

$$\begin{aligned} W(k) &= \cosh^{-1} \left\{ \frac{1}{J^2 - \gamma^2} [(J^2 + \gamma^2) \cosh(\beta \Delta) \right. \\ &\quad \left. + 4J\gamma(t \cos k - U) \sinh(\beta \Delta) \Delta^{-1}] \right\}, \\ A_y(k) &= -\sin k \frac{(J^2 - \gamma^2)^{\frac{3}{2}}}{J^2 + \gamma^2}, \\ A_z(k) &= t \cos k - U + \frac{J\gamma}{J^2 + \gamma^2} \frac{\Delta}{\tanh(\beta \Delta)}, \end{aligned} \quad (5)$$

captures the information of the quantum state in which the non-Hermitian system resides. Specific, this result implies that the quantum state of the non-Hermitian system is mapped to the quantum state of a Hermitian system with Hamiltonian H_{eff} at unit temperature.

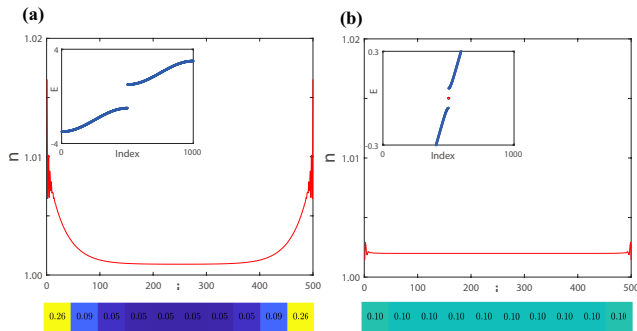


FIG. 3. (a) Particle distributions of the system. The upper plot illustrates the average quantity of particles per cell (number of cells is L , number of particles is $L + 1$). The lower rectangle signifies the distribution of particle number in a system fractioned into 10 regions. Parameters are set to $U = 2$, $T = 0.1$, $\gamma = J - \delta$. (b) Particle distributions given $U = 0$, $T = 0.15$, and $\gamma = -(J - \delta)$. All figures are examined under parameters $L = 500$, $\delta = 10^{-3}$, $t = 1$ and $J = 2$.

The phase transition point corresponds to the band closure point of H_{eff} . This model has zero mode when $U_{c-} < U < U_{c+}$. Based on the classification of the Hermitian model, this model has topology. Therefore, the critical point $U_{c\pm}$ is the topological phase transition point for the state of the non-Hermitian system. Therefore, the four regions in the phase diagram respectively represent the state of the system being in a topological phase and the energy band structure of the system being in a topological phase. To visualize the verification, we calculated the state density distribution and the energy band for Region II and Region III. In particular, the system exhibits a phase where the energy band structure is in a topological phase while the state structure is in a non-topological phase, as well as a phase where the energy band structure is in a non-topological phase while the state structure is in a topological phase, as shown in Fig. 3. In Fig. 3(a), the system do not exhibit a zero mode, but calculation of the particle density shows accumulation near the edges, indicating the existence of edge states. In contrast, in Fig. 3(b), while the system have a zero mode, there is no particle accumulation towards the edges—the particle density fluctuations at the boundary are a boundary effect which also present in topologically trivial Hermitian models and do not lead to an accumulation of particles at the edges.

The above result implies that the many-body non-Hermitian systems need to be characterized by a pair of topological invariants (W, w) , which respectively describe the topology of the energy bands and the quantum states. Such findings provoke us to inquire: What topological invariant is truly capable of predicting the topology of quantum states?

State topological invariant.—We construct a topological invariant to characterize the topology of quantum

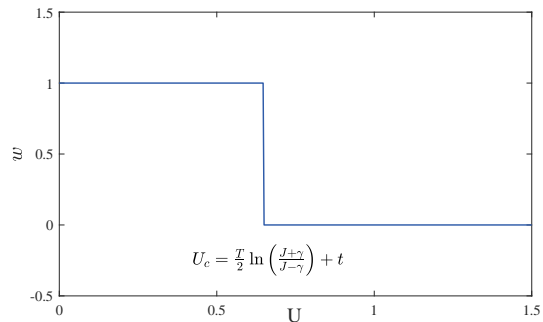


FIG. 4. Numerical result of the topological invariant. $t = 0.5$, $T = 0.1$, $J = 1$ and $\gamma = 0.9$.

states. Previous constructions use H_{NH} as the starting point, which should be revised to directly reflect the properties of the many-body quantum state. Therefore, the topology of the state for the non-Hermitian system is characterized by the topological invariant of system with Hamiltonian H_{eff} , which is defined as

$$w = \frac{1}{2\pi i} \int_{-\pi}^{\pi} dk \text{tr} \sigma_x H_{\text{eff}}^{-1} \frac{d}{dk} H_{\text{eff}}. \quad (6)$$

By calculating the winding number, we find that the change in the topological number does not occur at $U_{g\pm}$. Instead, the change occurs at $U_{c\pm} = \frac{T}{2} \ln \frac{J \pm \gamma}{J - \gamma} \pm t$. We have $w = 1$ for $U_{c-} < U < U_{c+}$ and $w = 0$ for $U > U_{c+}$ or $U < U_{c-}$, see Fig. 4. The transition of the topological number, the emergence of boundary states, and the location of phase transitions without gap closure, all align consistently. Therefore, we have identified the correct topological invariant for the system.

However, it should be noted that the definition of topological invariants is not use the topological number defined by 38-fold classification, and simply replace H_{NH} with H_{eff} . This system under different parameters, belongs to different symmetry classes of 38-fold classification, but the state characterised by the same topological invariant. When U and t are not all equal to zero, the system only exhibits chiral symmetry $\sigma_x H(k) \sigma_x = -H^\dagger(k)$. When $U = t = 0$, the system has an additional sub-lattice symmetry $\sigma_z H(k) \sigma_z = -H(k)$, but under these two parameters, the symmetry of its effective Hamiltonian is not increased, including the zero-temperature limit. The symmetry class is the AIII class. This means that the classification of states requires determining symmetry classes of non-Hermitian Hamiltonian in a way that is different from the 38-fold classification, and defining topological invariants that are associated with them.

Symmetric class and topological invariants for non-Hermitian system's states.—We deduce the symmetry class and topological invariants that dictate the topology of quantum states in non-Hermitian systems. The completion of the symmetric class can be based on the

following observation: while non-Hermitian systems have non-Hermitian Hamiltonians, their quantum states are invariably described by a Hermitian density matrix, thus, it can be characterized by an effective Hermitian Hamiltonian $\hat{H}_{\text{eff}} \equiv \ln \rho$. Here ρ is the steady-state density matrix. Apart from direct calculations, the density matrix can be determined by the statistical mechanics of non-Hermitian systems, which is described in the supplementary Materials [35]. The effective Hermitian is classification by the AZ symmetry classes, which are defined by the presence or absence of time-reversal symmetry, particle-hole symmetry, or chiral symmetry, and essentially consists of 10 distinct categories. Consequently, the core issue in obtaining the symmetry class of the effective Hamiltonian is how to map the symmetry class of the non-Hermitian Hamiltonian of the many-body non-Hermitian systems. The following theorem provides the first step to solve this problem:

Theorem 1: The Hamiltonian of a non-Hermitian system \hat{H}_{NH} and the system's effective Hamiltonian \hat{H}_{eff} exhibit the following relation, i.e., $\hat{G}\hat{H}_{\text{NH}}\hat{G}^{-1} = \hat{H}_{\text{NH}}$ if and only if $\hat{G}(\exp \hat{H}_{\text{eff}})\hat{G}^\dagger = \exp \hat{H}_{\text{eff}}$, where \hat{G} denotes a linear operator (for finite temperature situations, the system-environment coupling also needs commuting with \hat{G}).

The proof of the theorem is provided in the supplementary material. This theorem can be interpreted as for linear operators, there is no ‘‘symmetry breaking’’ in the system—that is, the Hamiltonian and states share the same symmetries. If \hat{G} is a unitary operator, we can take the logarithm on both sides of the equation satisfied by \hat{H}_{eff} , resulting in \hat{H}_{NH} and \hat{H}_{eff} sharing the same unitary symmetries. Noteworthy, in the conventional topological classification of non-Hermitian systems, there exist certain extended symmetries, manifest in non-Hermitian Hamiltonians such as the sublattice symmetry $\hat{S}\hat{H}\hat{S}^{-1} = \hat{H}^\dagger$, which are not reflected in the effective Hamiltonian. An example has already been discussed at the end of the previous section.

Theorem 1 illustrates that the PHS can be mapped from the effective Hamiltonian symmetry of the non-Hermitian system to the Hamiltonian's symmetry. However, both TRS and CS required for the AZ classification are anti-unitary symmetries and also anti-linear, therefore this theorem is not applicable for these symmetries. Although for the models considered in Eq. (1), the chiral symmetry σ_x is simultaneously preserved in non-Hermitian Hamiltonians and effective Hamiltonians, this preservation isn't always present. An example of this ineffectiveness can be considered the scenario where $\hat{H}'_{\text{NH}} = (1 + i)\hat{H}_{\text{NH}}$. In this situation, the system will linger on the state with the largest imaginary part, a condition analogous to the zero-temperature scenario in the case of real spectra. The effective Hamiltonian still exhibits chiral symmetry, but the Hamiltonian of the system will change under the chiral symmetry. The cause

of this symmetry breaking resides in the fact that anti-unitary operators always transform gaining states into dissipative states. The anti-unitary symmetry in the Hamiltonian represents a constraint between the gain and loss states, while the presence of anti-unitary symmetry in the effective Hamiltonian implies certain constraints on the ground state itself. These are not the same requirement, hence the conclusion that anti-unitary symmetry cannot be mapped between the effective Hamiltonian and the system Hamiltonian.

To take into account anti-unitary symmetries, we define the linearized operator \hat{G}_L^A of anti-unitary operator \hat{G}^A . Its action on the Hamiltonian \hat{H}_{NH} is defined as

$$\hat{G}_L^A \hat{H}_{\text{NH}} (\hat{G}_L^A)^{-1} \equiv (\hat{G}^A)_{\{|n\rangle_R\}} \hat{H}_{\text{NH}} (\hat{G}^A)_{\{|n\rangle_R\}}^{-1}, \quad (7)$$

Here $(\hat{G}^A)_{\{|n\rangle_R\}} \equiv \sum_n (\hat{G}^A |n\rangle_R) \langle n|_L$ with $\{|n\rangle_R\}$, $\{|n\rangle_L\}$ is the set of biorthogonal left and right eigenstates of the Hamiltonian \hat{H}_{NH} . The operator \hat{G}_L^A is referred to as ‘‘linearized’’ because its action on operators satisfies linear in multiplication by arbitrary complex number. When acting on the effective Hamiltonian corresponding to the steady-state ensemble ρ of a system with Hamiltonian \hat{H}_{NH} , we have [36]

$$\hat{G}_L^A (\exp \hat{H}_{\text{eff}}) (\hat{G}_L^A)^\dagger = \hat{G}^A (\exp \hat{H}_{\text{eff}}) (\hat{G}^A)^{-1}. \quad (8)$$

Since $(\hat{G}^A)_{\{|n\rangle_R\}}$ is a linear operator, the Theorem 1 can be applied. Combining on Eqs. (7) and (8), we obtain that:

Theorem 2: The effective Hamiltonian of a non-Hermitian system has a symmetry \hat{G}_L^A if and only if the system's Hamiltonian has symmetry \hat{G}_L^A .

The conditions for a single-particle Hamiltonian to satisfy linearized TRS (LTRS) and linearized CS (LCS) are [36]

$$\begin{aligned} T_L H_{\text{NH}}^* T_L^{-1} &= \text{Re} H_{\text{NH}} - i \text{Im} H_{\text{NH}} \\ \Gamma_L H_{\text{NH}}^\dagger \Gamma_L^{-1} &= -\text{Re} H_{\text{NH}} + i \text{Im} H_{\text{NH}}, \end{aligned} \quad (9)$$

where T_L , Γ_L are single-particle unitary operator, $\text{Re} H_{\text{NH}}$ is defined as sharing the same eigenstates with H_{NH} , but with eigenvalues corresponding to the real part of H_{NH} 's eigenvalues. Similarly, the operator is defined as sharing the same eigenstates with H_{NH} , but with eigenvalues corresponding to the imaginary part of H_{NH} 's eigenvalues. We define the square of the linear operator as the square of these first quantization operators T_L and Γ_L . It can be proved that $T_L^2 = \hat{T}^2$ and $\Gamma_L^2 = \hat{\Gamma}^2$, where $\hat{T}, \hat{\Gamma}$ are the original time-reversal operator and chiral operator. When the Hamiltonian has a real spectrum, we can note that the linearized symmetry is equivalent to the original symmetry. This implies that both unitary and anti-unitary symmetries of the system's Hamiltonian can be mapped to the symmetry of the system's effective Hamiltonian under real spectrum scenarios, consistent with the examples presented in this paper. The

two types of symmetries become non-equivalent when the Hamiltonian of the system has a complex spectrum.

Based on the above discussions, we have obtained the topological classification table for non-Hermitian systems, see Table I.

Class	LTRS	PHS	LCS	$d = 1$	$d = 2$	$d = 3$
A	0	0	0	0	Z	0
AI*	+1	0	0	0	0	0
AII*	-1	0	0	0	Z_2	Z_2
AIII*	0	0	1	Z	0	Z
BDI*	+1	+1	1	Z	0	0
CII*	-1	-1	1	Z	0	Z_2
D	0	+1	0	Z_2	Z	0
C	0	-1	0	0	0	Z
DIII*	-1	+1	1	Z_2	Z_2	Z
CI*	+1	-1	1	0	0	Z

TABLE I. Topological classification of many-body non-Hermitian systems in 1-3 dimensions.

The topological invariants for Table I can be derived. For classes A, D, C the topological invariant is nothing but that defined in the AZ symmetry class, only the Hamiltonian needs to be replaced with the effective Hamiltonian. For other classes that are marked as X*, the topological invariant is substituting the effective Hamiltonian into the topological invariant of the corresponding AZ symmetry class X.

It's worth noting that there are systems with non-Hermitian skin effect [37–54]. The density matrix of the systems does not have translational symmetry under open boundary conditions [55]. For a Hermitian system, topology can only be well defined for systems with translational invariance, which leads to the topology of the systems with skin effect not being well-defined.

Conclusions.—In this letter, we find that in non-Hermitian systems, state's topological phase transitions occur at points where the gap does not close at finite temperature case. This implies that the topology of states and energy bands appear separately, and the previous works only describe the emergence of energy bands topology. We discover that the topology of states are determined by the topological invariant of the symmetry class that combines the Hamiltonian with particle-hole symmetry, linearized time-reversal symmetry, and linearized chiral symmetry. These identified topological invariants accurately predict the topology of states. Our research unveils a unique facet of many-body non-Hermitian systems. Investigations into this unique behavior create an exciting avenue for future explorations.

This work was supported by the Natural Science Foundation of China (Grants No. 11974053 and No. 12174030).

* Corresponding author; spkou@bnu.edu.cn

- [1] B. A. Bernevig, T. L. Hughes, and S.-C. Zhang, Quantum Spin Hall Effect and Topological Phase Transition in HgTe Quantum Wells, *Science* **314**, 1757 (2006).
- [2] L. Fu, C. L. Kane, and E. J. Mele, Topological Insulators in Three Dimensions, *Phys. Rev. Lett.* **98**, 106803 (2007).
- [3] J. E. Moore and L. Balents, Topological Invariants of Time-Reversal-Invariant Band Structures, *Phys. Rev. B* **75**, 121306(R) (2007).
- [4] L. Fu and C. L. Kane, Topological Insulators with Inversion Symmetry, *Phys. Rev. B* **76**, 045302 (2007).
- [5] X.-L. Qi, T. L. Hughes, and S.-C. Zhang, Topological Field Theory of Time-Reversal Invariant Insulators, *Phys. Rev. B* **78**, 195424 (2008).
- [6] R. Roy, Topological Phases and the Quantum Spin Hall Effect in Three Dimensions, *Phys. Rev. B* **79**, 195322 (2009).
- [7] M. König, S. Wiedmann, C. Brüne, A. Roth, H. Buhmann, L. Molenkamp, X.-L. Qi, and S.-C. Zhang, Quantum Spin Hall Insulator State in HgTe Quantum Wells, *Science* **318**, 766 (2007).
- [8] M. Z. Hasan and C. L. Kane, Colloquium: Topological Insulators, *Rev. Mod. Phys.* **82**, 3045 (2010).
- [9] X.-L. Qi and S.-C. Zhang, Topological Insulators and Superconductors, *Rev. Mod. Phys.* **83**, 1057 (2011).
- [10] N. Read and D. Green, Paired States of Fermions in Two Dimensions with Breaking of Parity and Time-Reversal Symmetries and the Fractional Quantum Hall Effect, *Phys. Rev. B* **61**, 10267 (2000).
- [11] A. Y. Kitaev, Unpaired Majorana Fermions in Quantum Wires, *Phys. Usp.* **44**, 131 (2001).
- [12] D. A. Ivanov, Non-Abelian Statistics of Half-Quantum Vortices in p-Wave Superconductors, *Phys. Rev. Lett.* **86**, 268 (2001).
- [13] L. Fu and C. L. Kane, Superconducting Proximity Effect and Majorana Fermions at the Surface of a Topological Insulator, *Phys. Rev. Lett.* **100**, 096407 (2008).
- [14] M. Sato, Y. Takahashi, and S. Fujimoto, Non-Abelian Topological Order in s-Wave Superfluids of Ultracold Fermionic Atoms, *Phys. Rev. Lett.* **103**, 020401 (2009);
- [15] J. D. Sau, S. Tewari, R. M. Lutchyn, and S. D. Sarma, Generic New Platform for Topological Quantum Computation Using Semiconductor Heterostructures, *Phys. Rev. Lett.* **104**, 040502 (2010); R. M. Lutchyn, J. D. Sau, and S. D. Sarma, Majorana Fermions and a Topological Phase Transition in Semiconductor-Superconductor Heterostructures, *Phys. Rev. Lett.* **105**, 077001 (2010).
- [16] Y. Oreg, G. Refael, and F. von Oppen, Helical Liquids and Majorana Bound States in Quantum Wires, *Phys. Rev. Lett.* **105**, 177002 (2010).
- [17] J. Alicea, Y. Oreg, G. Refael, F. von Oppen, and M. P. A. Fisher, Non-Abelian Statistics and Topological Quantum Information Processing in 1D Wire Networks, *Nat. Phys.* **7**, 412 (2011).
- [18] J. Alicea, New Directions in the Pursuit of Majorana Fermions in Solid State Systems, *Rep. Prog. Phys.* **75**, 076501 (2012).
- [19] M. Sato and Y. Ando, Topological Superconductors: A Review, *Rep. Prog. Phys.* **80**, 076501 (2017).
- [20] Altland and M. R. Zirnbauer, Nonstandard Symmetry Classes in Mesoscopic Normal-Superconducting Hybrid

- Structures, Phys. Rev. B **55**, 1142 (1997)
- [21] X. Chen, Z.-C. Gu, and X.-G. Wen, Local unitary transformation, long-range quantum entanglement, wave function renormalization, and topological order, Phys. Rev. B **82**, 155138 (2010).
- [22] S. Sachdev, *Quantum Phase Transitions* (Cambridge University Press, Cambridge, England, 2001).
- [23] E. H. Lieb and D. W. Robinson, The finite group velocity of quantum spin systems, Commun. Math. Phys. **28**, 251 (1972).
- [24] M. B. Hastings and T. Koma, Spectral gap and exponential decay of correlations Commun. Math. Phys. **265**, 781 (2006).
- [25] B. Nachtergaele and R. Sims, Lieb-Robinson bounds and the exponential clustering theorem, Commun. Math. Phys. **265**, 119 (2006).
- [26] P. Schnyder, S. Ryu, A. Furusaki, and A. W. W. Ludwig, Classification of Topological Insulators and Superconductors in Three Spatial Dimensions, Phys. Rev. B **78**, 195125 (2008).
- [27] A. Kitaev, Periodic Table for Topological Insulators and Superconductors, AIP Conf. Proc. **1134**, 22 (2009).
- [28] C.S. Ryu, A. P. Schnyder, A. Furusaki, and A. W. W. Ludwig, Topological Insulators and Superconductors: Tenfold Way and Dimensional Hierarchy, New J. Phys. **12**, 065010 (2010).
- [29] K. Kawabata, S. Higashikawa, Z. Gong, Y. Ashida, and M. Ueda, Topological Unification of Time-Reversal and Particle-Hole Symmetries in Non-Hermitian Physics, Nat. Commun. **10**, 297 (2019).
- [30] K. Kawabata, K. Shiozaki, M. Ueda, and M. Sato, Symmetry and Topology in Non-Hermitian Physics, Phys. Rev. X **9**, 041015 (2019)
- [31] H. Zhou and J. Y. Lee, Periodic Table for Topological Bands with Non-Hermitian Symmetries, Phys. Rev. B **99**, 235112 (2019)
- [32] N. Matsumoto, K. Kawabata, Y. Ashida, S. Furukawa and M. Ueda, Continuous phase transition without gap closing in non-Hermitian quantum many-body systems, Phys. Rev. Lett. **125**, 260601 (2020).
- [33] F. Yang, H. Wang, M.-L. Yang, C.-X. Guo, X.-R. Wang, G.-Y. Sun and S.-P. Kou, Hidden continuous quantum phase transition without gap closing in non-Hermitian transverse Ising model, New J. Phys. **24**, 043046 (2022).
- [34] Z. Gong, Y. Ashida, K. Kawabata, K. Takasan, S. Higashikawa, and M. Ueda, Topological Phases of Non-Hermitian Systems, Phys. Rev. X **8**, 031079 (2018).
- [35] K. Cao and S.-P. Kou, Statistical mechanics for non-Hermitian quantum systems, Phys. Rev. Res. **5**, 033196 (2023).
- [36] See Supplemental Material.
- [37] S. Yao and Z. Wang, Edge states and topological invariants of non-Hermitian systems, Phys. Rev. Lett. **121**, 086803 (2018).
- [38] S. Yao, F. Song and Z. Wang, Non-Hermitian Chern bands, Phys. Rev. Lett. **121**, 136802 (2018).
- [39] F. K. Kunst, E. Edvardsson, J. C. Budich and E. J. Bergholtz, Biorthogonal bulk-boundary correspondence in non-Hermitian systems, Phys. Rev. Lett. **121**, 026808 (2018).
- [40] C. Yin, H. Jiang, L. Li, R. Lü and S. Chen, Geometrical meaning of winding number and its characterization of topological phases in one-dimensional chiral non-Hermitian systems, Phys. Rev. A **97**, 052115 (2018).
- [41] C. H. Lee and R. Thomale, Anatomy of skin modes and topology in non-Hermitian systems, Phys. Rev. B **99**, 201103 (2019).
- [42] K. Yokomizo and S. Murakami, Non-bloch band theory of non-hermitian systems, Phys. Rev. Lett. **123**, 066404 (2019).
- [43] K. Zhang, Z. Yang and C. Fang, Correspondence between winding numbers and skin modes in non-Hermitian systems, Phys. Rev. Lett. **125**, 126402 (2020).
- [44] D. S. Borgnia, A. J. Kruchkov and R.-J. Slager, Non-Hermitian boundary modes and topology, Phys. Rev. Lett. **124**, 056802 (2020).
- [45] Y. Yi and Z. Yang, Non-Hermitian skin modes induced by on-site dissipations and chiral tunneling effect, Phys. Rev. Lett. **125**, 186802 (2020).
- [46] L. Li, C. H. Lee, S. Mu and J. Gong, Critical non-Hermitian skin effect, Nat. Commun. **11**, 5491 (2020).
- [47] N. Okuma and M. Sato, Non-hermitian skin effects in hermitian correlated or disordered systems: Quantities sensitive or insensitive to boundary effects and pseudo-quantum-number, Phys. Rev. Lett. **126**, 176601 (2021).
- [48] F. Roccati, Non-Hermitian skin effect as an impurity problem, Phys. Rev. A **104**, 022215 (2021).
- [49] K. Zhang, Z. Yang and C. Fang, Universal non-Hermitian skin effect in two and higher dimensions, Nat. Commun. **13**, 2496 (2022).
- [50] E. Lee, H. Lee and B.-J. Yang, Many-body approach to non-Hermitian physics in fermionic systems, Phys. Rev. B **101**, 121109 (2020).
- [51] S. Mu, C. H. Lee, L. Li and J. Gong, Emergent Fermi surface in a many-body non-Hermitian fermionic chain, Phys. Rev. B **102**, 081115 (2020).
- [52] T. Liu, J. J. He, T. Yoshida, Z.-L. Xiang and F. Nori, Non-Hermitian topological Mott insulators in one-dimensional fermionic superlattices, Phys. Rev. B **102**, 235151 (2020).
- [53] D.-W. Zhang, Y.-L. Chen, G.-Q. Zhang, L.-J. Lang, Z. Li and S.-L. Zhu, Skin superfluid, topological Mott insulators, and asymmetric dynamics in an interacting non-Hermitian Aubry-André-Harper model, Phys. Rev. B **101**, 235150 (2020).
- [54] Z. Xu and S. Chen, Topological Bose-Mott insulators in one-dimensional non-Hermitian superlattices, Phys. Rev. B **102**, 035153 (2020).
- [55] K. Cao, Q. Du, and S.-P Kou, Many-body non-Hermitian skin effect at finite temperatures, Phys. Rev. B **108**, 165420 (2023).